PFC/RR-81-20

DOE/ET/51013-20

MATTED FIBER DIVERTOR TARGETS FOR SPUTTER RESISTANCE

P.J. Gierszewski
N.E. Todreas
B. Mikic
T.F. Yang

June 1981

Research supported by DOE contract #DE-AC02-78ET-51013

MATTED FIBER DIVERTOR TARGETS FOR SPUTTER RESISTANCE

P.Gierszewski
N.E. Todreas
B. Mikic
T.F. Yang

Abstract

Reductions in net sputtering yields can be obtained by altering the surface topography to maximize redeposition of sputtered atoms. A simple analysis is used to indicate a potential reduction by a factor of 2 to 5 for matted fiber divertor targets, relatively independent of incident, reflected and sputtered atom distributions. The fiber temperature is also shown to be acceptable, even up to 10 MW/m^2, for reasonably combinations of materials, fiber diameter and fiber spacing.

MATTED FIBER DIVERTOR TARGETS FOR SPUTTER RESISTANCE

1.0 Introduction

The customary approach to decreasing sputtering from surfaces exposed to a given flux of energetic plasma ions is to look for sputter-resistant materials. Here we consider the advantages gained by using a matted fiber surface to intercept the plasma - ie. optimizing the geometry to reduce the net outflow of sputtered atoms. The fundamental assumption is that the sputtered atoms will redeposit if they strike a surface again shortly after the primary sputtering event. Thus we try to design a surface that maximizes the probability of a sputtered atom striking another facet of the surface rather than escaping back into the plasma.

Ziegler et al [1] proposed altering the surface microtopography by depositing a dense array of single crystal whiskers. They anticipated a reduction in sputtering because: (1) most sputtered atoms would be released down into the whiskers; (2) orientation of the crystal axes could promote channeling rather than a sputtering cascade; and (3) preferential sputtering at grain boundaries would be reduced. Their experimental results with tungsten whiskers (up to 80 μm high) in 4 keV He^+ discharges showed a reduction in net sputtering yield by a factor of 3 to 100.

Cramer and Oblow [2,3] considered altering the surface macro-topography by using a honeycomb vacuum wall. Sputtered atoms produced inside the honeycomb cells were presumed likely to strike the cell walls and redeposit. They ran Monte Carlo codes to determine net sputtering yield as a function of depth/diameter, incident ion distribution, reflection probabilities and reflection distributions. A general reduction by a factor of 2 to 4 was found, with little improvement beyond a depth/diameter ratio of about unity.

In this paper, we consider the potential sputtering reduction from a matted fiber target (structurally similar to steel wool, for example). The idea is to maximize the depth of penetration of the primary ion before the sputtering event occurs. Then the sputtered atom has a reasonable chance of redepositing as opposed to simply escaping from the target (Figure 1). If there is a sputtering reduction, then this scheme could be mechanically simpler to construct or replace than honeycomb walls or microwhiskers - one can even imagine a roll which is slowly unravelled across the divertor target surface. It is also relatively insensitive (because of the random orientation of the fiber surfaces) to the incident ion angle. In subsequent sections, we consider the potential sputtering reduction and heat transfer capabilities of this concept.

2.0 Sputter resistance

Consider a fiber volume fraction α. If the average fiber spacing is p, then over a distance p the probability of interacting is roughly A_f/A where A_f is the normal surface area covered by fibers and A is the total exposed normal area. Since $\alpha \sim (A_f p/Ap)$, we can approximate the ion attenuation (for many incident ions) as a continuous curve with a characteristic mean free path $\lambda \sim p/\alpha$. But

$$\alpha \sim (\pi d^2/4)/(\pi p^2/4) = (d/p)^2 \tag{1}$$

where d is the fiber diameter. So

$$\lambda \sim d/\alpha^{3/2} \tag{2}$$

and the ion flux is, where x is distance into target,

$$\phi(x) \sim \phi_0 e^{-x/\lambda} \tag{3}$$

This should be a reasonable approximation for $\lambda >> p$ ($\alpha << 1$).

In a region x to x+dx, the interaction rate is

$$d\phi = -\phi(x)\, dx/\lambda \tag{4}$$

If the sputtering coefficient for plasma ions on the solid material is S_o (atoms/ion), then the gross sputtering rate per unit normal area is

$$dR(x) = S_o\, |d\phi| = S_o\, \phi_o\, e^{-x/\lambda}$$

or

$$R = \int_0^t \frac{S_o \phi_o e^{-x/\lambda}}{\lambda}\, dx \tag{5}$$

where t is the matted fiber target thickness.

If all these sputtered atoms escaped from the target, then the net sputtering coefficient is

$$S_{net} = \frac{R}{\phi_o} = S_o \int_0^t \frac{e^{-x/\lambda}}{\lambda}\, dx \tag{6}$$

In practice, t will be sufficiently large to stop all ions, so we take $t \to \infty$ with small error. Then

$$S_{net} \sim S_o \int_0^\infty e^{-x/\lambda}\, d(x/\lambda) = S_o \tag{7}$$

This is the usual result for a flat solid surface.

Now consider the possibility that atoms sputtered at a depth x may strike a surface on their way back out and redeposit. The incident ion is taken as having an angle θ with the surface normal vector and a normalized incident distribution $f(\theta)$. The sputtered atoms come off at an angle ϕ with the surface and have a normalized emission distribution $g(\phi)$ (see Figure 2). So

$$\int_0^{\pi/2} f(\theta)\, d\theta = 1 \tag{8}$$

$$\int_0^{\pi} g(\phi)\, d\phi = 1 \tag{9}$$

These sputtered atoms have a path length $y = x/\cos(\Theta+\phi-\pi/2)$ back to the surface. They will attenuate along this distance according to $e^{-y/x}$, assuming redeposition when they contact another fiber. Since the incident plasma ion energies are around 1 keV, the sputtered atoms should be much less energetic after allowing for collisional momentum transfer between light and heavy atoms, multiple collisions per ion, and surface binding energies, depending upon the process. Experimental data on energy spectra of sputtered particles is summarized by Kraus and Wright [4]. Self-sputtering yields scale as S_{self} (atoms/ion) $\sim 0.001\ E(eV)$ for energies below about 1 keV [5], so $S_{self} < 0.01$ atoms/ion for $E < 10$ eV. Hence we expect almost complete redeposition from the sputtered atoms inside the target.

For practical targets, the area will be much larger than λ so the mat can be considered infinite in the horizontal dimensions. Then the net sputtering coefficient is

$$S_{net} \sim \frac{1}{\phi_o} \int_0^\infty w(x)\ dR(x) \qquad (10)$$

where

$$w(x) = \int_0^{\pi/2} f(\Theta)\ S'(\Theta) \int_0^{\pi-\theta} g(\phi)\ e^{-x/\lambda\cos(\theta+\phi-\pi/2)}\, d\phi\ d\theta$$

This $w(x)$ weights the sputtering rate to account for redeposition, and $S'(\theta) = S_{actual}/S_o$ allows for variation in sputtering yield with incident angle. Note that sputtered atoms travelling away from the surface ($\theta+\phi>\pi$) are assumed unlikely to reach the surface since they would redeposit rather than reflect from deeper fibers.

We can determine S_{net} for a variety of incident and sputtered distributions. In general, $f(\Theta)$ should be constant - ie. $f(\Theta) = 2/\pi$. This is true, for example, with a random arrangement of fibers, or if the fiber surface is rough. $S'(\theta)$ can be estimated as (Figure 3)

$$S'(\theta) \sim 1/\cos\theta \qquad \theta < 80° \qquad (11)$$

For $\theta < 80°$, the incident ions are simply reflected. (Note that 80° is only approximate, and increases with ion energy.) The biggest uncertainty is in $g(\phi)$, the emission angular distribution. Three possibilities are considered here - peaking at a particular angle, roughly away from the incident ion's path, and random.

Consider the simplest possibility first - emission at a particular angle ϕ. Some data (Figure 4) suggests that $g(\phi)$ is peaked at about 30° from the surface normal vector. We model this possibility as $g(\phi) \sim \delta(2\pi/3)$ where $\delta(\phi)$ is the delta function. Then

$$w(x) = \int_0^{\pi/3} \frac{2}{\pi} \frac{e^{-x/\lambda\cos(\Theta+\pi/6)}}{\cos\Theta} \, d\Theta \qquad (12)$$

where the upper limit on θ is now $\pi/3$, consistent with the $\theta+\phi < \pi$ requirement. Then

$$S_{net} = \int_0^{\infty} \frac{S_o}{\lambda} e^{-x/\lambda} \cdot \frac{2}{\pi} \int_0^{\pi/3} \frac{e^{-x/\lambda\cos(\theta+\pi/6)}}{\cos\theta} \, d\theta \, dx$$

$$= \frac{2S_o}{\pi} \int_0^{\pi/3} \frac{\cos(\theta+\pi/6)}{[1+\cos(\theta+\pi/6)]} \, d\theta \qquad (13)$$

Expanding $\cos(\theta+\pi/6)$ and letting $z = \tan(\theta/2)$,

$$S_{net} = \frac{4S_o}{\pi} \int_0^{0.58} \frac{(0.866-z-0.866z^2)\, dz}{(1-z^2)(1.866-z+0.134z^2)} = 0.23\, S_o \qquad (14)$$

This result is independent of λ because $t >> \lambda$ assumed.

And if the assumption that $g(\phi) \sim \delta(2\pi/3)$ is too unrealistic, consider the alternate case of isotropic emission over $\phi = \pi/2$ to π, $g(\phi) \sim 2/\pi$. Then

$$w(x) = \frac{2}{\pi} \int_0^{\theta_{max}} \int_{\pi/2}^{\pi-\theta} \frac{2}{\pi} \frac{e^{-x/\lambda\cos(\theta+\phi-\pi/2)}}{\cos\theta} \, d\theta \, d\phi \qquad (15)$$

Here θ_{max} is limited to less than 90° since, at some energy-dependent

angle, the incident ions simply reflect and do not sputter. For hydrogenic ions around 1 keV, $\theta_{max} \sim 80°$ or $(8/9)(\pi/2)$. These reflected ions are still travelling deeper into the mat and can still give rise to sputtered atoms. We model these by increasing the effective penetration mean free path λ by a factor 9/8. So

$$S_{net} = \frac{4S_o}{\pi^2\lambda} \int_0^{\infty} \int_{\pi/2}^{4\pi/9} \int_{\pi-\theta}^{} \frac{e^{-(x/\lambda)[8/9+1/\cos(\theta+\phi-\pi/2)}}{\cos\theta} d\theta d\phi dx$$

$$= \frac{4S_o}{\pi^2} \int_0^{4\pi/9} \int_{\pi/2}^{\pi-\theta} \frac{\cos(\theta+\phi-\pi/2)\ d\theta\ d\phi}{[1 + 8/9\ \cos(\theta+\phi-\pi/2)]\ \cos\theta}$$

$$= \frac{4S_o}{\pi^2} \int_0^{4\pi/9} \frac{d\theta}{\cos\theta} \int_0^{\pi/2} \frac{\cos\psi\ d\psi}{1 + 8/9\ \cos\psi}$$

$$= \frac{4S_o}{\pi^2} \int_0^{4\pi/9} \frac{[0.599-1.125\theta+4.911\tan^{-1}(0.2425\tan\theta/2)]\ d\theta}{\cos\theta} \quad (16)$$

Since θ varies over 0 to $4\pi/9$, then $\tan^{-1}(0.2425\ \tan\theta/2) \sim 0.2425\ \tan\theta/2$ to within 2%. So

$$S_{net} = S_o \int_0^{1.396} \frac{0.2426 - 0.4559\ \theta + 0.4827\ \tan\theta/2}{\cos\theta} d\theta$$

$$= 0.21\ S_o \quad (17)$$

A third possibility is $g(\phi) \sim 1/\pi$, random (isotropic) emission over $\phi = 0$ to π. This assumes that the sputtered atom's direction is completely independent of the incident ion. The solution is similar to Eqns. (15) to (17), and the result is $S_{net} = 0.40\ S_o$.

All these calculations suggest $S_{net} \sim 0.2$ to $0.4\ S_o$. This agrees with Cramer and Oblow who obtained 0.2 to $0.5\ S_o$ (over a wide range of incident, reflected and sputtered atom distributions) for their honeycomb wall design with depth/diameter greater than unity.

One approximation in the present equations is that atoms travelling back near the incident ion's path are numerically attenuated, when the path should be clear. For $\lambda >> p$ (ie. $\alpha << 1$) and for $f(\theta)$ and $g(\phi)$ not peaked back along the incident ion's path, the magnitude of this error should be small.

Another approximation is that the ions are assumed to only cause sputtering at their first impact point. If they also reflect, it is assumed that their energy is too low to cause further sputtering. Cramer and Oblow modelled this multiple sputtering by using a reflection probability at each interaction, and found that allowing a reflection probability of as much as 50% increased S_{net} by up to 50% (from 0.2 to 0.3 S_o, for example).

The conclusion from these simple calculations is that changes in surface shape such as a matted fiber target can reduce net sputtering yield by a factor of 2 to 5, reasonably independent of the exact distribution of the incident, reflected and sputtered atoms.

3.0 Heat transfer across a matted fiber

While a matted fiber target may be a simple passive scheme to get reductions of up to 80% in sputtering yield, it must be able to handle high energy fluxes to be useful in divertor applications. In principle, the fibers can be designed sufficiently free to allow thermal expansion and thus be insensitive to fatigue, yet sufficiently intertwined to provide a reasonably short path along the fibers to the cooled substrate. And since the fibers need carry little mechanical load, the limit is vaporization of the hottest fibers.

Treat the mat as having an effective thermal conductivity, $k_{eff} \sim \alpha k_o$, where k_o is the thermal conductivity of the solid material and α accounts for the internal voids. Experimental results in the limit of large fiber volume fraction ($\alpha \sim 0.7 - 1.0$) indicate this approximation is optimistic by up to a factor of 2 [6,7], but it should give reasonable scaling.

In steady-state with an internal exponential heat source, the temperature difference across the mat is slightly less than if the heat is all deposited at the surface, so

$$T_{fo} - T_{fi} \sim q''t/k_{eff} \qquad (18)$$

where T_{fo} and T_{fi} are the average outer and inner fiber temperatures, and q'' is the incident energy flux.

We have assumed $t >> \lambda$ so all ions are stopped in the mat, but heat transfer dictates t be as small as possible. We take $t \sim 10\lambda$ as a compromise. But $\lambda \sim d/\alpha^{3/2}$ (Eqn. 2) so

$$T_{fo} - T_{fi} \sim \frac{10\ d\ q''}{\alpha^{5/2}\ k_o} \tag{19}$$

Since heat is conducted along the fibers, the hottest point is actually the midpoint of exposed fibers on the mat outer surface. The temperature rise over a length L of a thin fiber under a uniform heat load q' (W/m) is

$$\Delta T_f \sim \frac{2q'L^2}{\pi d^2 k_o} \tag{20}$$

Depending on the fiber orientation, $q' \leq q''d$.

To estimate L, consider the intertwined fibers as approximately bounding "cubes" of $(2L)^3$ volume. Thus the hottest point is a distance L from each corner. From the definition of fiber volume fraction, and since each fiber is shared by four cubes,

$$\alpha = \frac{\text{fiber volume}}{\text{cube volume}} \sim \frac{1/4 \times 12 \times \pi d^2/4 \times 2L}{(2L)^3} = 0.6\,\frac{d^2}{L^2} \tag{21}$$

Since the hottest fiber point is at the mat temperature rise Eqn.(19) plus the exposed fiber temperature rise Eqn.(20),

$$T_{fo,max} - T_{fi} \sim \frac{q''d}{\alpha k_o}\left[\frac{10}{\alpha^{3/2}} + 0.4\right] \tag{22}$$

Some representative results are given in Table 1. These show that reasonable temperatures are possible for $d < 1$ mm, $\alpha \sim 0.25$ to 0.50, and $k_o > 100$ W/m-K, even at $q'' = 10$ MW/m^2. We emphasise that these conclusions are based on simple analysis, and do not include an accurate fiber mat thermal conductivity or on the other hand, for example, possible convective and radiative heat transfer across neutral gas within the fiber volume.

It is likely that some fibers will have conduction path lengths longer than estimated in Eqn.(21) unless the mat is carefully manufactured. However, these will (if too long) vaporize until the remaining length can handle the heat load, implying some shakedown to steady-state operation.

If the temperatures are still too high, a second approach is to use overlaid wire screens as opposed to random fibers. Again we produce a porous surface for the incident ions, but the space between the fibers, and so the conduction heat path, is decreased - ie. $\alpha \sim A_f/A$ still, but now $\lambda \sim d/\alpha$. This reduces the temperature drop across the mat by $\alpha^{1/2}$, or more than 30% for $\alpha < 0.5$.

4.0 Conclusions

The matted fiber divertor target concept has been shown by simple analysis to result in a decrease in net sputtering yield by up to a factor of 5 over a flat surface. Heat transfer by conduction alone may allow reasonable temperatures even at 10 MW/m^2 in materials like molybdenum, tungsten or copper, but there is considerable uncertainty in the effective heat transfer across the fiber mat.

5.0 References

1. J.F. Ziegler, J.J. Cuomo and J. Roth, 'Reduction of ion sputtering yield by special surface microtopotraphy', App. Phys. Lett., 30(6), 268 (1977).
2. S.N. Cramer and E.M. Oblow, 'Feasibility study of a honeycomb vacuum wall for fusion reactors', Nucl. Fus., 15, 339 (1975).
3. S.N. Cramer and E.M. Oblow, 'Reduction of re-fluxing neutral particles into a CTR plasma by use of a honeycomb wall', Nucl. Fus., 16, 158 (1976).
4. A.R. Kraus and R.B. Wright, 'Energy and mass distribution of sputtered particles', Journal of Nucl. Mat., 89(2&3), 229 (1980).
5. M. Gordinier, 'The impact of plasma wall interactions on the burn dynamics of tokamak reactors', UWFDM-356, University of Wisconsin, May 1980.
6. T. Takahashi and T. Kikuchi, 'Porosity dependence on thermal diffusivity and thermal conductivity of lithium oxide Li_2O from 200 - 900°C', Journal of Nucl. Mat., 91, 93 (1980).
7. H. Matsuo, 'Effect of porosity on thermal conductivity of nuclear graphite', Journal of Nucl. Mat., 89(1), 9 (1980).

Table 1: Representative temperature rises across matted fiber targets at q" = 10 MW/m^2

Material	k_o (W/m-K)	ΔT (K) d = 0.2 mm α=0.25	d = 0.2 mm 0.50	d = 1.0 mm 0.50	d = 1.0 mm 0.75	T_{melt} (K)
316SS	21	31000	5500	27000	10000	1640
V	37		3100			2170
Nb	90		1300			2690
Mo	110	5800	1000	5200	1900	2880
W	120		960			3680
Al	210		550			930
Cu	400	1600	290	1400	530	1360

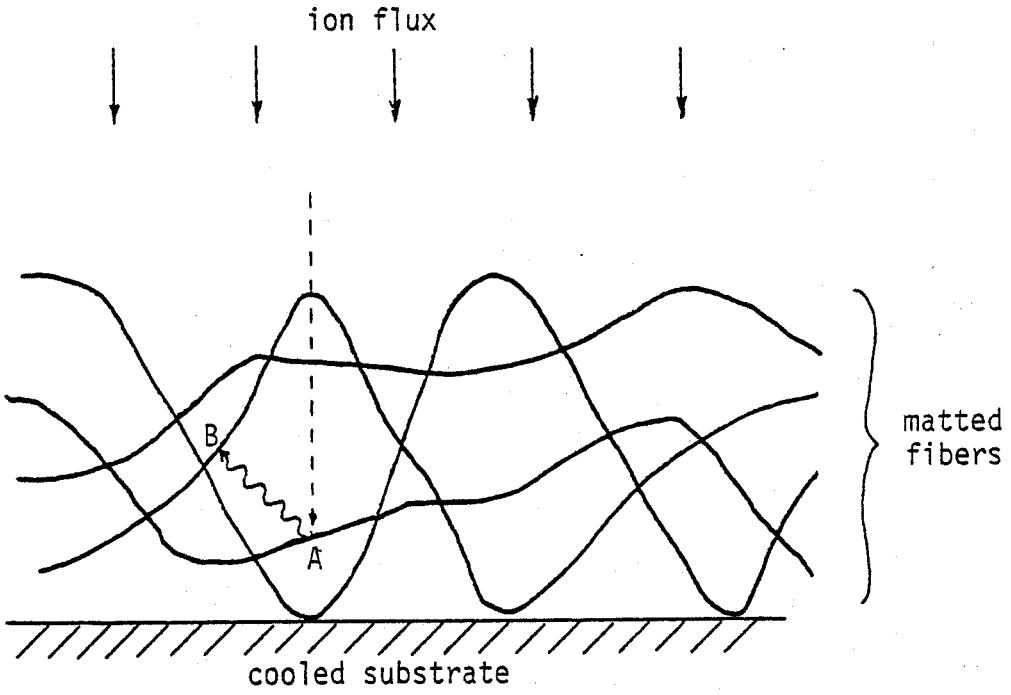

Figure 1: Matted fiber divertor target illustrating sputtering event at A with subsequent redeposition of sputtered atom at B.

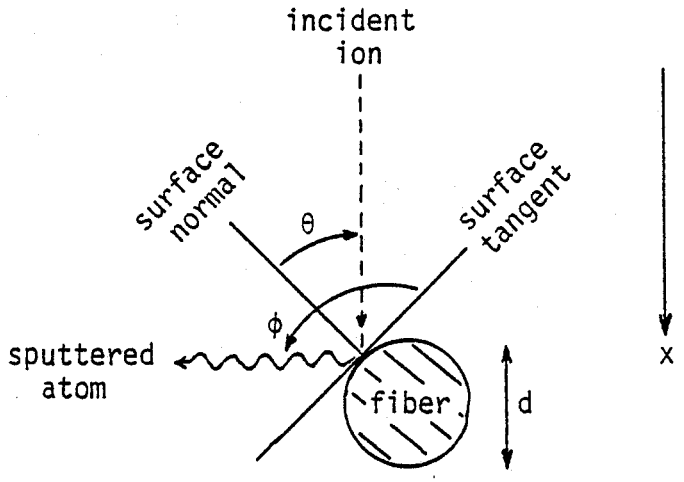

Figure 2: Definition of incident ion and sputtered atom angles.

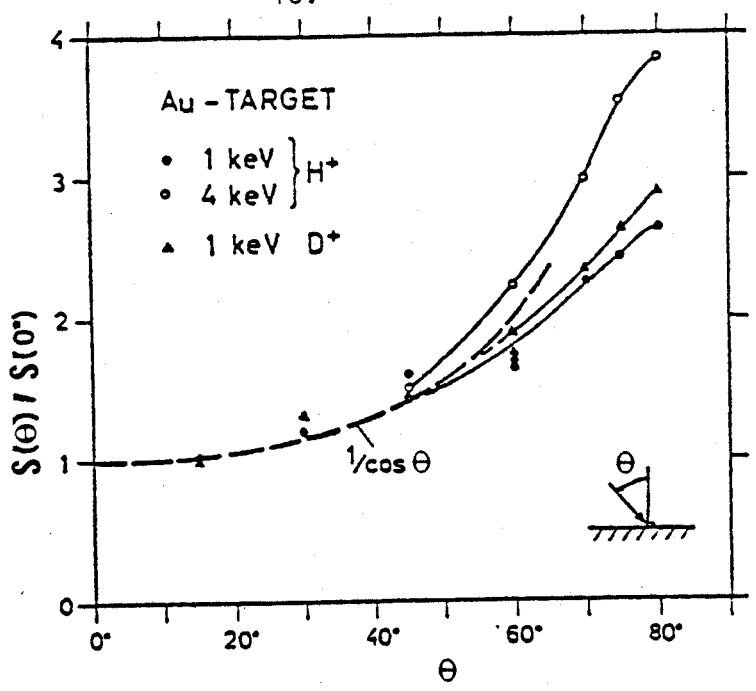

Figure 3: Sputtering yield as a function of incident ion angle with the surface normal vector. (taken from Ref.5)

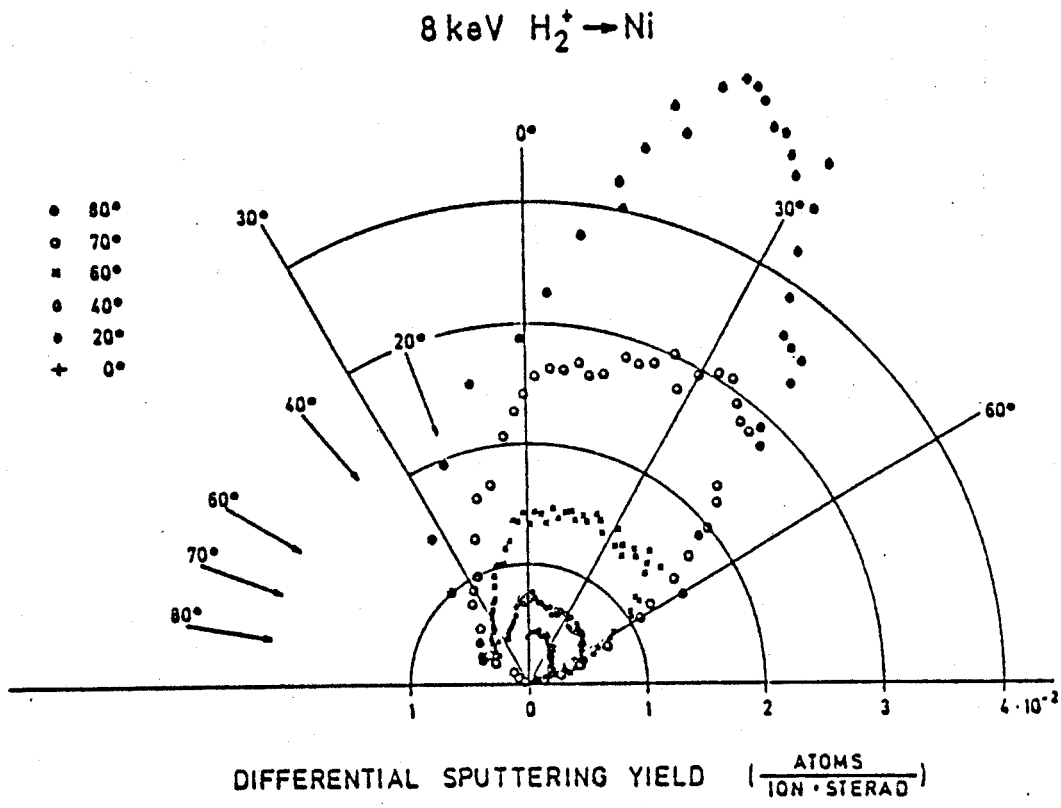

Figure 4: Sputtering yield and angular distribution as a function of incident ion angle with surface normal. (taken from Ref.5)